19 p.

N64 13188*
CODE-1
(NASA CR-55139)
OTS: $1.60 ph, $0.80 mf

UARI RESEARCH REPORT NO. 5

NON-EQUILIBRIUM HYPERSONIC FLOW OF AIR IN HYPERSONIC NOZZLES AND AROUND BLUNT BODIES

OTS PRICE
XEROX $ 1.60 ph.
MICROFILM $ 0.80 mf

Janardanarao Yalamanchili, and Thoenes
Rudolf Hermann, and Jurgen

Aug. 1963 19 p. ref.

Condensed Version of U A R I Research Report No. 3

prepared by

Jurgen Thoenes

Paper presented at the 5th International Symposium on Space Technology and Science, (ISTS) at Tokyo, Japan, September 2 - 7, 1963

This research work is partially supported by Army Material Command (AMCPM-ZER-R) under research contract No. DA-01-009-AMC-18(Z) and is also partially supported by National Aeronautics and Space Administration under the research grant NsG-381.

(NASA Grant NsG-381)

U.
UNIVERSITY OF ALABAMA RESEARCH INSTITUTE
Huntsville, Alabama

August 1963

U A R I Research Report No. 5

NON-EQUILIBRIUM HYPERSONIC FLOW OF AIR IN HYPERSONIC NOZZLES AND AROUND BLUNT BODIES

by

Janardanarao Yalamanchili
Rudolf Hermann

Condensed Version of U A R I Research Report No. 3

prepared by

Jurgen Thoenes

Paper presented at the Fifth International Symposium on Space Technology and Science (ISTS) at Tokyo, Japan, September 2 - 7, 1963

This research work was partially supported by the Army Materiel Command (AMCPM-ZER-R) under research contract No. DA-01-009-AMC-18(Z) and was also partially supported by NASA under the research grant NsG-381.

UNIVERSITY OF ALABAMA RESEARCH INSTITUTE

Huntsville, Alabama

August 1963

ABSTRACT

13188

Non-equilibrium hypersonic nozzle flow of air is investigated for supply temperatures of 4000 to 6000°K, supply pressures of 10 to 100 atm and for nozzle area ratios of 1 to 10,000.

The direct method is used for the first time to calculate the non-equilibrium hypersonic flow of air around blunt bodies. Results are given for the flow around a circular cylinder.

AUTHOR

NOMENCLATURE

A	Area
A^*	Nozzle throat area
C	Number of free or combined oxygen atoms per unit mass of air ($1.2886 \cdot 10^{26}$ atoms/slug)
h	Enthalpy
K_e	Equilibrium constant
k_r	Recombination rate constant, $(Ft^3/particle)^2\ sec^{-1}$
M	Mach number
$\dot{m}$	Mass flow
n_{02}	Number of oxygen particles per unit volume of undissociated air
n_{N2}	Number of nitrogen particles per unit volume of undissociated air
p	pressure
R	Gas constant of undissociated air
r	radial coordinate
T	Temperature (^oK)
U	Velocity (ft/sec)
x	distance along nozzle
Z	Compressibility factor
α	degree of oxygen dissociation
ϵ	dimensionless shock detachment distance
θ	angular coordinate
ρ	density ($slugs/ft^3$)
σ	shock angle

Subscripts

b	body surface
o	stagnation conditions behind the shock
s	downstream side of shock
t	supply conditions
∞	free stream conditions

Introduction

In the expansion of high enthalpy air in hypersonic nozzles, where the state changes are generally very rapid, it is possible that collision frequencies may be insufficient to maintain molecular vibration, dissociation, electronic excitation or even ionization in local thermodynamic equilibrium. In this event, the state of the air after an expansion in the nozzle to hypersonic speeds can be very different from the equilibrium state which is desired for the simulation of flight conditions of a re-entering body, both with respect to thermodynamic and gas dynamic variables as well as local chemical composition. In the first part of this investigation, an attempt has been made to solve the equations for one-dimensional flow of high enthalpy air through a hypersonic nozzle with oxygen dissociation over a wide range of temperatures and pressures. The results were obtained by using an IBM-7090 computer of the Marshall Space Flight Center at Huntsville, Alabama. The second part of this investigation is concerned with the determination of the flow field of dissociated air between the shock and a blunt body in hypersonic flow by the so-called direct method. This method was first suggested by Dorodnitsyn and was later developed by Belotserkovskii for an ideal gas flow around a sphere and a cylinder. Because of the complexity of the problem that we have to master in applying the direct method to the dissociated flow around a blunt body, the flow around a circular cylinder is considered here. Also, only the first approximation is solved and it is assumed that the results converge very rapidly as it was shown for an ideal gas by Belotserkovskii.

Chapter 1

High Temperature Air Flow in Hypersonic Nozzles

1.1 Basic Assumptions and Equations.

The one-dimensional steady nozzle flow calculations are based on the following assumptions:

1) Viscosity, diffusion and heat conduction of air are neglected.

2) The constituents of dissociated air are assumed to be thermally perfect.

3) The internal energies due to translational, rotational and vibrational degrees of freedom of the participating species are assumed to be those pertaining to thermal equilibrium. The range of densities and temperatures is restricted such that ionization can be neglected.

4) Radiation is neglected.

5) The model of the air that is considered consists only of O, O_2 and N_2.

The basic equations are the equation of state which is specialized to meet the employed model of the air, the momentum equation, the energy equation, the continuity equation and the rate equation. In the expression for the enthalpy the internal energy is assumed to be the weighted sum of the internal energies of each component due to translational, rotational and vibrational degrees of freedom, plus the dissociation energy of oxygen. The rate equation describes the dissociation and recombination process of the oxygen molecules or atoms, respectively, and relates the local chemical composition to the usual flow variables.

1.2 Non-equilibrium Flow in the Hypersonic Nozzle.

Because of the low velocity in the subsonic portion of the nozzle, the flow is assumed to be in equilibrium up to the throat. Assuming an isentropic expansion, the temperature, compressibility factor and the enthalpy can be determined from a Mollier Chart for arbitrary values of the pressure. The corresponding density and velocity can then be calculated. The throat conditions can be found by either comparing the velocity and the speed of sound or by calculating the mass flux which must be a maximum at the throat. The throat conditions determined by this procedure represent the initial values for the non-equilibrium flow in the supersonic portion of the nozzle.

From the five basic equations we can now derive three differential equations with three unknowns, namely α, ρ, and T. These equations are

$$\frac{d\alpha}{dx} = \frac{C^2\rho^2\left(1+\frac{n_{02}}{n_{02}+n_{N2}}\right)k_r\left[\frac{K_e}{2C}(1-\alpha)-\rho\alpha^2\right]}{2\left(\frac{n_{02}}{n_{02}+n_{N2}}\right)\left(\frac{\dot{m}}{A^*}\right)\left(\frac{A^*}{A}\right)} \tag{1.1}$$

$$\frac{d\rho}{dx} = \frac{RZT\left(\frac{A}{A^*}\right)^2\rho^3\left[\frac{1}{Z}\left(\frac{n_{02}}{n_{02}+n_{N2}}\right)\frac{d\alpha}{dx}+\frac{1}{T}\frac{dT}{dx}-\left(\frac{A^*}{A}\right)\frac{d}{dx}\left(\frac{A}{A^*}\right)\right]}{\left(\frac{\dot{m}}{A^*}\right)^2(1-K)}$$

$$-\rho\left(\frac{A^*}{A}\right)\frac{d}{dx}\left(\frac{A}{A^*}\right) \tag{1.2}$$

$$\text{where } K = \frac{RZT\rho^2\left(\frac{A}{A^*}\right)^2}{\left(\frac{\dot{m}}{A^*}\right)^2}$$

$$\frac{dT}{dx} = \frac{(1-K)\left[\frac{\partial h}{\partial\alpha}-\frac{RT}{1-K}\left(\frac{n_{02}}{n_{02}+n_{N2}}\right)\right]\frac{d\alpha}{dx}+RZT\left(\frac{A^*}{A}\right)\frac{d}{dx}\left(\frac{A}{A^*}\right)}{RZ-\frac{\partial h}{\partial T}(1-K)} \tag{1.3}$$

Specifying in addition the shape of the nozzle as a function of X, the above differential equations are simultaneously solved on a high speed IBM-7090 computer by the third order Runge-Kutta integration method. In order to start the numerical integration, the derivatives at the throat are specified to be those of equilibrium flow. This is justified because of the small interval of integration that was chosen.

1.3 Numerical Results of the Nozzle Flow Calculations.

As observed by Bray for Lighthill's ideally dissociated gas, freezing of the chemical composition occurs just downstream of the throat (Fig. 1). This can be explained by the fact that dissociation and recombination processes, which are balanced at the equilibrium reservior conditions, decrease at different rates as the air expands. In particular, the rate of dissociation tends to zero first, decreasing exponentially with temperature and thereby leaving the recombination as the net reaction. The $d\alpha/dx$ approaches rapidly zero as the gas expands because it is

proportional to the square of the density. It is interesting to note that the temperature distribution (Fig. 2) is influenced considerably by non-equilibrium flow effects, particularly at higher (A/A*), which indirectly influences the Mach number. Generally the calculations show that the velocity is not sensitive to non-equilibrium effects. The pressure is lower than the equilibrium value, while the density is not much effected. It was also found that the nozzle shape has practically no effect on the various flow parameters.

Chapter 2

Non-Equilibrium Hypersonic Flow Around Blunt Bodies

2.1. Inverse and Direct Methods.

The practical importance of blunted shapes in the hypersonic flight of an object re-entering from outer space has led to many recent investigations of hypersonic flow with detached shock waves, using both inverse and direct methods. In the inverse method the flow field around the body is determined by specifying a certain shock shape. The associated body shape follows then from the calculation. The problems associated with the specification of boundary conditions along an unknown shock are thus avoided and this method has been successfully applied by Hall, even for real gas flows. However, this method is rather difficult if applied to the flow around bodies with a varying surface curvature.

Recently, Dorodnitsyn has described an iteration procedure for the solution of two-dimensional boundary value problems. This method is also applicable to problems with free boundaries and has been applied by Belotserkovskii to the supersonic flow of an ideal gas past a circular cylinder. This basic work has been reviewed by Holt and extended by various authors, Traugott for example, but it has not yet been applied to blunt body flows in a real gas. In this investigation it is attempted to calculate the flow field around a circular cylinder in dissociated air by this integral method, but the equations are given in the proper form both for the sphere and the circular cylinder. Numerical calculations were done for the cylinder on the GE-225 computer of the Marshall Space Flight Center at Huntsville, Alabama.

2.2 Basic Assumptions and Equations.

The calculation of the blunt body flow is based on the same assumptions that were given for the nozzle flow in section 1.1. However, there are now two independent variables, namely the radial coordinate r and the angular coordinate θ. Using these polar coordinates, referred to the center of the cylinder, the equations of motion can all be written as partial differential equations in r and θ:

$$\frac{\partial F}{\partial r} + \frac{\partial G}{\partial \theta} + H = 0$$

where F, G, and H are functions of all the flow variables.

Before eq. (2.1) can be integrated between the shock and the body surface, shock transition conditions have to be determined, i.e. we have to find expressions for the derivatives of all flow variables with respect to θ. These derivatives are derived under the following assumptions:

1) The shock is assumed to be locally an oblique shock.

2) The composition of the gas does not change across the shock.

It is furthermore assumed that for hypersonic flow $p_\infty \ll \rho_\infty Un_\infty^2$, and also that the contribution of the free stream temperature to the enthalpy can be neglected, not, however, the energy bound in the free stream dissociation.

2.3. Application of Belotserkovskii's Method for the Flow Past a Circular Cylinder.

Having reduced the equations of motion to the form of eq. (2.1), Belotserkovskii's method consists essentially of transforming the partial differential equations with two independent variables into ordinary differential equations with one variable. Integrating eq. (2.1) with respect to r between the body surface (r_b) and the shock surface (r_s) we get eq. (2.2):

$$(F)_s - (F)_b + \int_{r_b}^{r_s} \frac{\partial G}{\partial \theta}\, dr + \int_{r_b}^{r_s} H\, dr = 0 \qquad (2.2)$$

Using Leibniz's formula for differentiating integrals, the second term on the left hand side can be rewritten and eq. (2.2) becomes eq. (2.3):

$$(F)_s - (F)_b + \frac{d}{d\theta} \int_{r_b}^{r_s} G\, dr - (G)_s \frac{dr_s}{d\theta} + \int_{r_b}^{r_s} H\, dr = 0 \qquad (2.3)$$

In order to integrate the equations of this form all integrands are now approximated by means of an interpolation polynomial in r. In our case only a first order polynomial is used and therefore the procedure is called the first approximation. Substituting the polynomial, introducing a dimensionless shock detachment distance ϵ and performing the integration, all equations assume the form of eq. (2.4):

$$(F)_s - (F)_b + \frac{r_b}{2}\frac{d\epsilon}{d\theta}\left[(G)_b + (G)_s\right] + \frac{\epsilon r_b}{2}\frac{d}{d\theta}\left[(G)_s - (G)_b\right]$$

$$+ \frac{\epsilon r_b}{2}\left[(H)_s - (H)_b\right] = 0 \qquad (2.4)$$

Using the previously established shock transition conditions and a simple geometrical relation between the shock detachment distance ϵ and the shock angle σ, the six equations of motion are now brought into the final form of eq. (2.5):

$$\phi_1 \frac{du_{\theta b}}{d\theta} + \phi_2 \frac{d\rho_b}{d\theta} + \phi_3 \frac{dp_b}{d\theta} + \phi_4 \frac{dT_b}{d\theta} + \phi_5 \frac{d\sigma}{d\theta} + \phi_6 \frac{d\alpha_b}{d\theta} + \phi_7 = 0 \qquad (2.5)$$

The ϕ's are functions of all the thermodynamic and gas dynamic variables. In total we have seven ordinary differential equations for the seven unknowns $U_{\theta b}$, ρ_b, p_b, T_b, σ, α_b, and ϵ, which are simultaneously solved by the computer.

2.4. Non-Equilibrium Flow Past a Circular Cylinder by the Direct Method.

For the actual calculation procedure all our differential equations are made dimensionless by relating the variables to their corresponding free stream values. The conditions behind the shock at each value of θ are calculated from the oblique shock relations. It is also assumed that the flow is in equilibrium at the stagnation point. Hence, the initial conditions behind the shock and at the stagnation point are the same as those of equilibrium flow for a given free stream condition.

The numerical procedure consists of two parts. First, for every value of θ the derivatives of all the variables are calculated from the set of simultaneous differential equations by using determinants. Then the derivatives are integrated simultaneously by the Runge-Kutta integration method. It should be noted that the equations do not readily yield the shock detachment distance on the stagnation stream line. In order to find ϵ_o, a very tedious iteration procedure has to be used. This iteration has to be continued until an ϵ_o is found such that all the derivatives of the variables are continuous across the sonic line. The equations are very sensitive with respect to ϵ_o and it was found that the time for the iteration could be considerably reduced by starting it with an approximate value of ϵ_o. This approximate value was obtained from the perfect gas equation given by Hayes and Probstein, substituting an equilibrium flow density ratio across the shock.

2.5. Discussion of the Numerical Results.

Because of the limited time during which the computer is available, results have been obtained so far only for one set of free stream conditions. In this particular case, there is 70% of frozen oxygen dissociation and the free stream velocity is U_∞ = 12,150 ft/sec. These conditions were chosen in order to show the distinctive effect of non-equilibrium flow in a wind tunnel nozzle on the flow field around a blunt body.

The degree of oxygen dissociation is almost constant up to the sonic line (Fig. 3), but is in the entire flow field up to the sonic point about 30% below the equilibrium value. It is interesting to note that the temperature, as in the non-equilibrium nozzle flow, is considerably lower than the equilibrium value when the sonic point is approached (Fig. 4). The pressure distribution is very close to the one predicted by the modified Newtonian theory. The most important results of the blunt body flow calculations are the shock shape and the shock detachment distance (Fig. 5). The shock shape deviates very much from the circle. Due to the free stream dissociation, the shock detachment distance is considerably increased if compared to perfect gas flow.

Conclusions

We have investigated high enthalpy, non-equilibrium nozzle flow of air. Results are given for supply temperatures of 4000 to 6000 ^{o}K and for supply pressures of 10 to 100 atmospheres. It is concluded that high temperature air flow in hypersonic wind tunnels is frozen because of the rapid expansion of the gas from the nozzle throat onward. This means that the chemical composition of the gas remains constant in the supersonic portion of the nozzle. This freezing has a strong effect on the temperature and the Mach number, but little effect on the pressure and vanishing effect on the density distribution along the nozzle.

The flow field around a circular cylinder up to the sonic point, the shock shape and the shock detachment distance are determined by the direct method. Shock shape and stand-off distance are very much affected by the frozen free stream dissociation, i. e. the shock moves further upstream and the shape deviates considerably from a circle. The degree of dissociation, the distribution of temperature, pressure and density in the flow field up to the sonic point are markedly different from those for equilibrium flow.

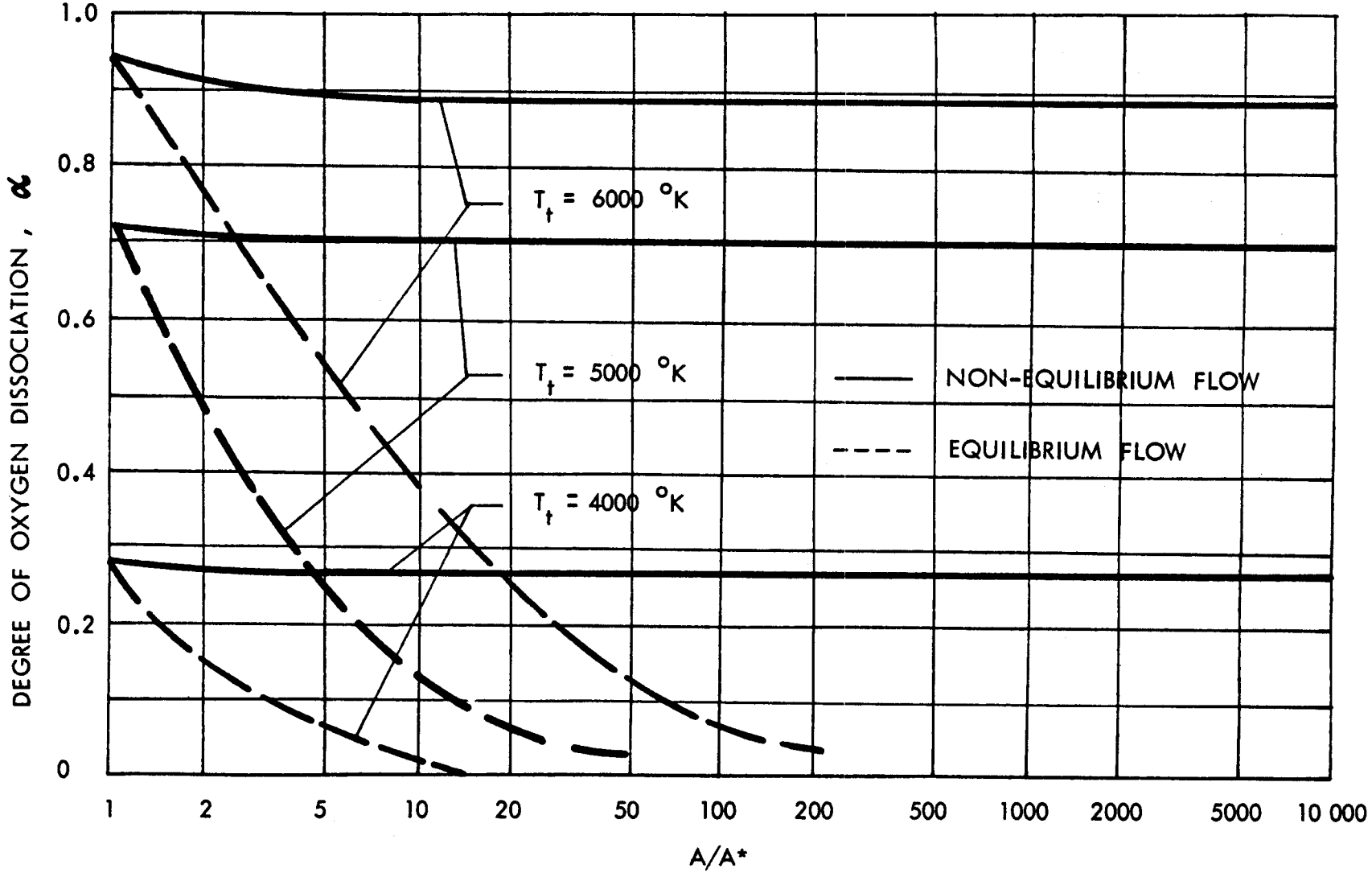

FIG. 1: DEGREE OF OXYGEN DISSOCIATION ALONG HYPERSONIC NOZZLE IN NON-EQUILIBRIUM FLOW FOR P_t = 10 atm

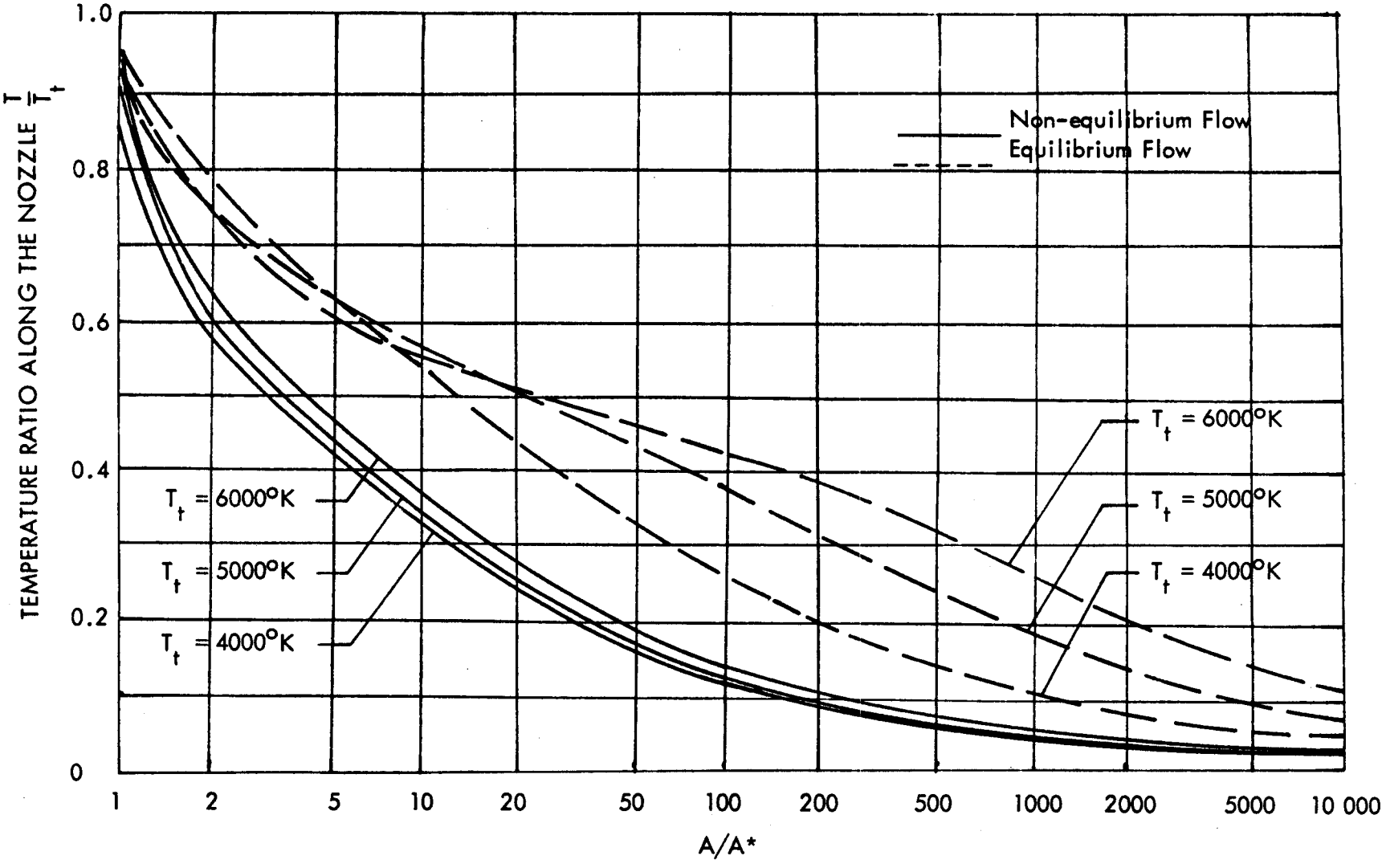

FIG. 2: TEMPERATURE DISTRIBUTION ALONG THE HYPERSONIC NOZZLE IN NON-EQUILIBRIUM FLOW FOR P_t = 10 atm

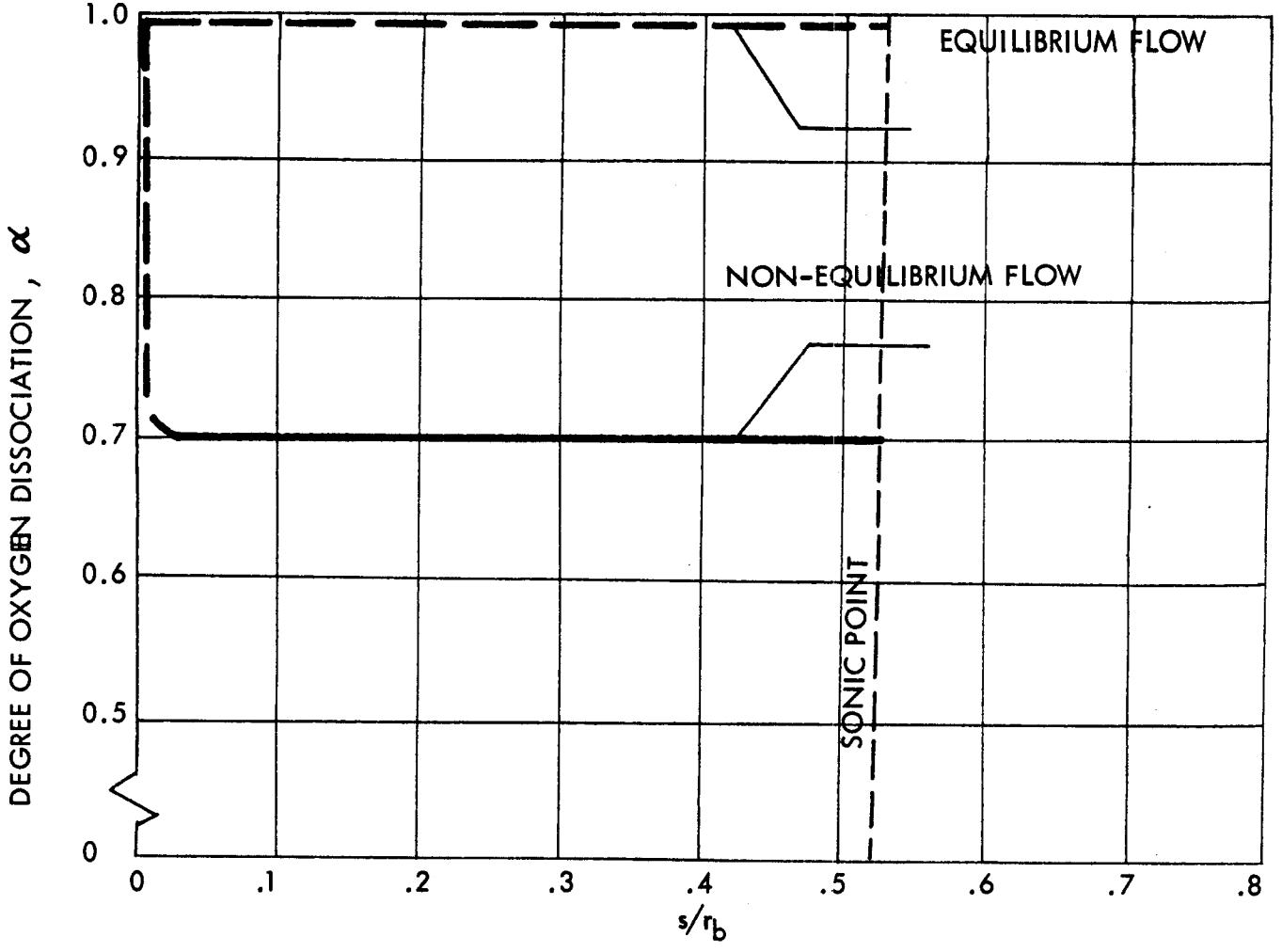

FIG. 3: DEGREE OF OXYGEN DISSOCIATION IN HYPERSONIC FLOW ON THE NON-REACTING SURFACE OF A CYLINDER IN A HYPERSONIC WIND TUNNEL ($M_f = 14.91$, $P_t = 10$ atm., $T_t = 5000^{\circ}K$)

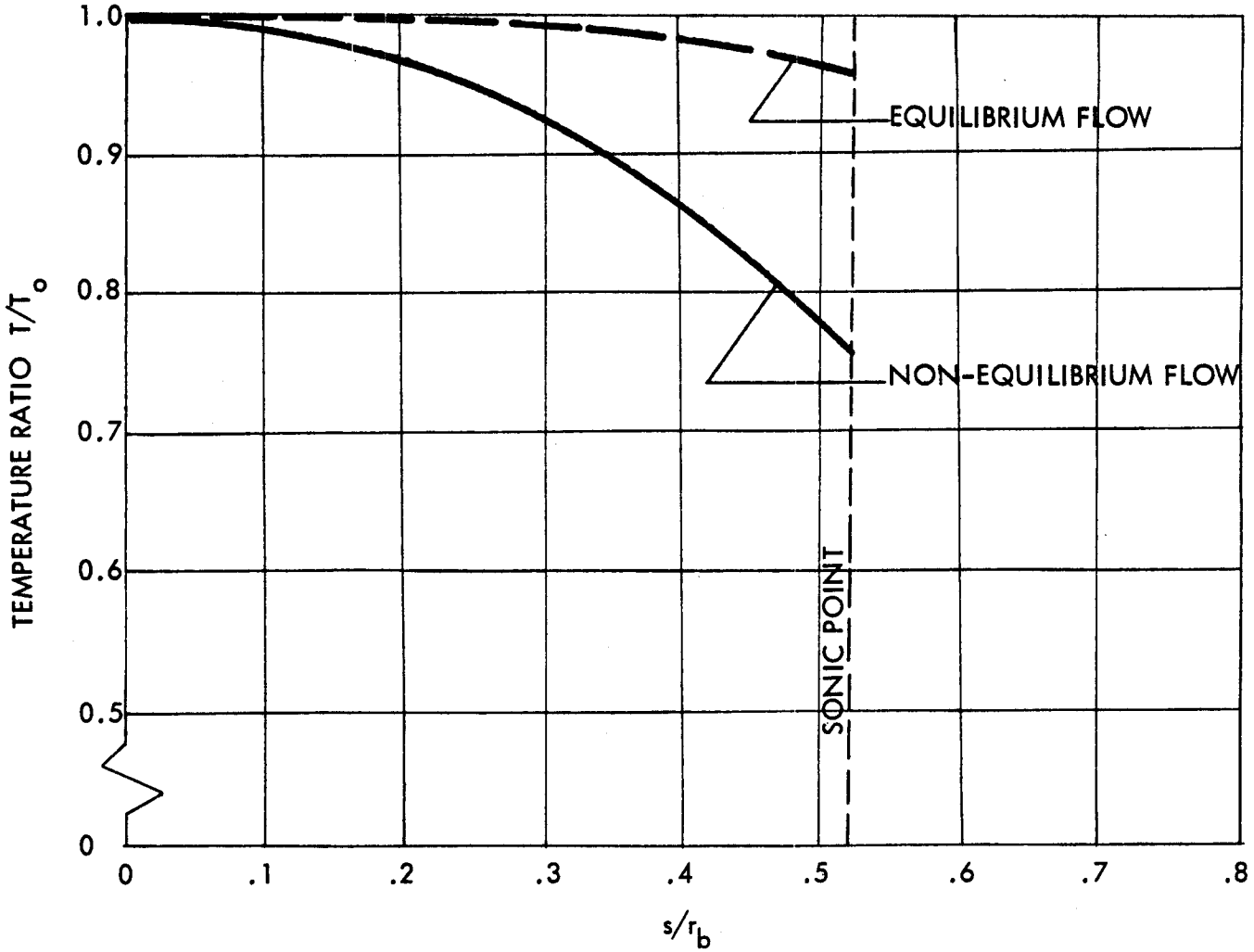

FIG. 4: TEMPERATURE DISTRIBUTION IN HYPERSONIC FLOW ON THE NON-REACTING SURFACE OF A CYLINDER IN A HYPERSONIC WIND TUNNEL ($M_f = 14.91$, $P_t = 10$ atm., $T_t = 5000°K$)

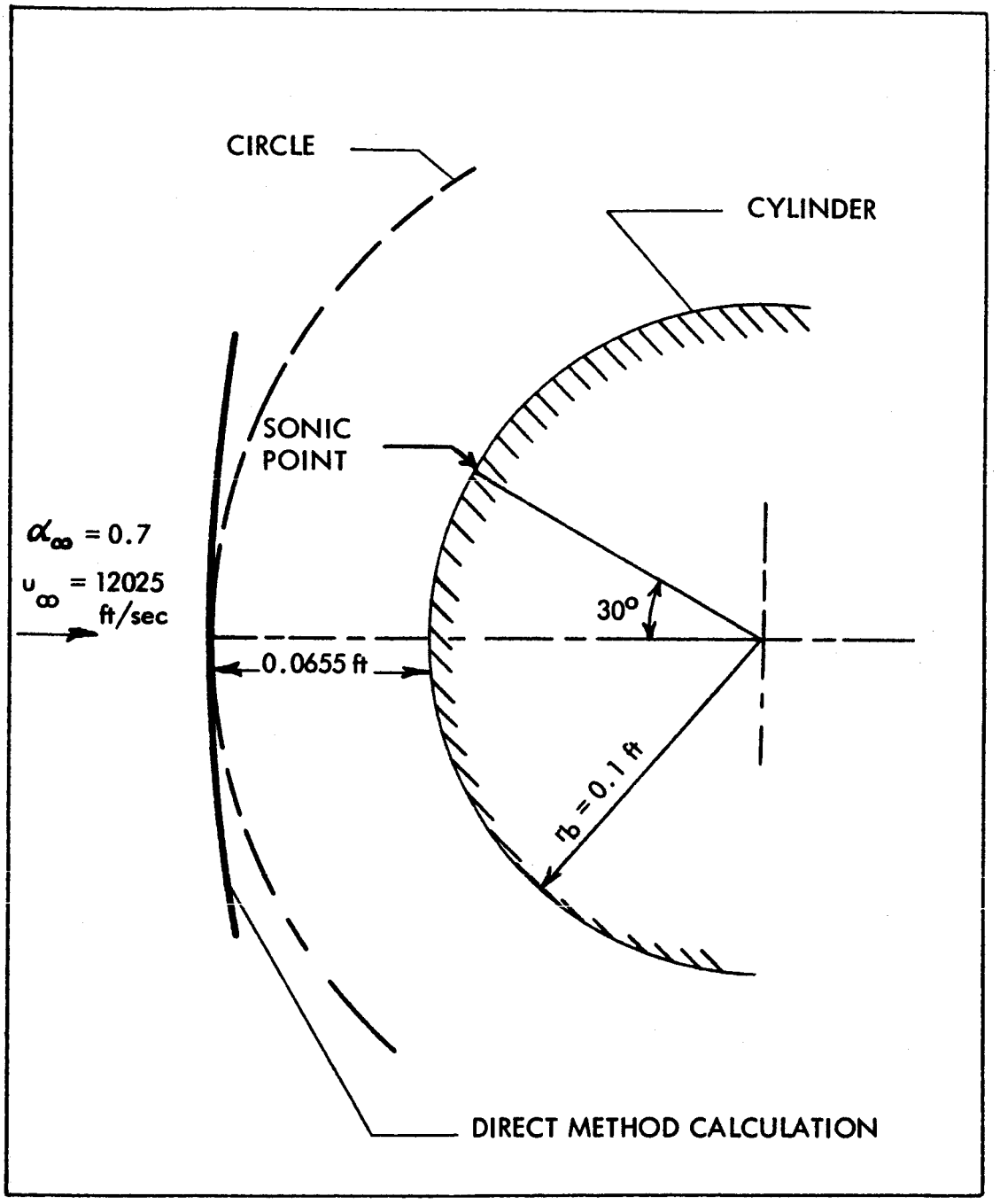

FIG. 5: CALCULATED SHOCK SHAPE BY DIRECT METHOD FOR NON-EQUILIBRIUM AIR FLOW AROUND A CYLINDER IN HYPERSONIC WIND TUNNEL. (M_f = 14.91, P_t = 10 atm., T_t = 5000°K)